Remote Aerosol Simulated During the Atmospheric Tomography (ATom) Campaign and Implications for Aerosol Lifetime

Chloe Yuchao Gao[1,2] , Colette L. Heald[1,3] , Joseph M. Katich[4,5,6] , Gan Luo[7] , and Fangqun Yu[7]

[1]Department of Civil and Environmental Engineering, Massachusetts Institute of Technology, Cambridge, MA, USA, [2]Now at Program in Atmospheric and Oceanic Sciences, Princeton University, Princeton, NJ, USA, [3]Department of Earth, Atmospheric and Planetary Sciences, Massachusetts Institute of Technology, Cambridge, MA, USA, [4]Cooperative Institute for Research in Environmental Sciences (CIRES), University of Colorado, Boulder, CO, USA, [5]NOAA Chemical Sciences Laboratory (CSL), Boulder, CO, USA, [6]Now at Ball Aerospace, Boulder, CO, USA, [7]Atmospheric Sciences Research Center, University at Albany, Albany, NY, USA

Abstract We investigate and assess how well a global chemical transport model (GEOS-Chem) simulates submicron aerosol mass concentrations in the remote troposphere. The simulated speciated aerosol (organic aerosol (OA), black carbon, sulfate, nitrate, and ammonium) mass concentrations are evaluated against airborne observations made during all four seasons of the NASA Atmospheric Tomography Mission (ATom) deployments over the remote Pacific and Atlantic Oceans. Such measurements over pristine environments offer fresh insights into the spatial (Northern [NH] and Southern Hemispheres [SH], Atlantic, and Pacific Oceans) and temporal (all seasons) variability in aerosol composition and lifetime, away from continental sources. The model captures the dominance of fine OA and sulfate aerosol mass concentrations in all seasons. There is a high bias across all species in the ATom-2 (NH winter) simulations; implementing recent updates to the wet scavenging parameterization improves our simulations, eliminating the large ATom-2 (NH winter) bias, improving the ATom-1 (NH summer) and ATom-3 (NH fall) simulations, but producing a model underestimate in aerosol mass concentrations for the ATom-4 (NH spring) simulations. Following the wet scavenging updates, simulated global annual mean aerosol lifetimes vary from 1.9 to 4.0 days, depending on species. Aerosol lifetimes in each hemisphere vary by season, and are longest for carbonaceous aerosol during the southern hemispheric fire season. The updated wet scavenging parameterization brings simulated concentrations closer to observations and reduces global aerosol lifetime for all species, indicating the sensitivity of global aerosol lifetime and burden to wet removal processes.

Plain Language Summary Aerosols are a key constituent of the atmosphere. Their lifetime in the atmosphere controls their global distribution and the resulting air quality and climate impacts. We use a global model (GEOS-Chem) to simulate their mass concentrations. To evaluate the model, we compare simulations against airborne measurements over the remote Pacific and Atlantic oceans made in all four seasons during the NASA Atmospheric Tomography Mission (ATom). The model generally reproduces organic and sulfate aerosols well, yet it over-estimates all species in the Northern Hemispheric (NH) winter season. An updated wet deposition method, which provides more effective aerosol removal, reduced the overestimation in this season, improved the simulation in NH summer and fall as well, but underestimated the concentrations in NH spring. With the model update, aerosol lifetimes vary from 1.9 to 4.0 days and by species and seasons, with organic aerosols and black carbon having the longest lifetime during the Southern Hemispheric fire season. The updated wet deposition scheme reduces these lifetimes significantly, demonstrating the sensitivity of aerosol lifetime and concentration to the wet removal process.

1. Introduction

Atmospheric aerosols directly and indirectly affect the radiative balance of the Earth; they are also key constituents of air pollution, exposure to which leads to the premature death of over 4 million people each year (Cohen et al., 2017; Seinfeld & Pandis, 2016). The chemical composition of aerosols and the processes that govern their life cycle are central to understanding their impact on air quality and climate. Understanding of global aerosol composition has advanced significantly in recent years in part due to the routine deployment of online

instrumentation in field campaigns. Despite these advancements, gaps and uncertainties remain in our knowledge of how different processes, for example, emissions, transport, and deposition, affect the aerosol lifetime and abundance.

The lifetime of aerosols represents, on average, how long particles stay in the atmosphere before they are removed. It dictates long-range transport, the intercontinental impact of aerosols, and ultimately the policy-relevant question of: What is the climate impact of a given emission? Early studies estimated that the lifetime of aerosols ranges from 4 to 60 days (Giorgi & Chameides, 1986; Graustein & Turekian, 1986; Martell & Moore, 1974), with shorter lifetimes associated with aerosols confined in source regions and longer lifetimes for long-range transported aerosols (Balkanski et al., 1993). For inorganic aerosols, AeroCom Phase III models exhibit global mean lifetimes of 2–7.8 days (mean of 5 days) for nitrate, 1.9–9.8 days (mean of 4.3 days) for ammonium, and 0.86–7.6 days (mean of 4.5 days) for sulfate (Bian et al., 2017; Park et al., 2004). Tsigaridis et al. (2014) reported that the global mean lifetime of organic aerosol (OA) ranges from 3.8 to 9.6 days (mean of 5.7 days) across the AeroCom Phase II models. Pai et al. (2020) estimated the OA lifetime simulated by GEOS-Chem at 4.9 and 5.8 days for two different schemes. To supplement the AeroCom studies, X. Liu et al. (2012) calculated aerosol lifetimes using the modal aerosol module (MAM 3 and MAM7), which includes aerosol microphysics, in the atmospheric component (CAM5) of the Community Earth System Model (CESM1). The more complex MAM7 reported sulfate lifetime at 3.8 days, ammonium at 3.4 days, primary organic matter (POM) at 5 days, secondary organic aerosol (SOA) at 4.1 days, and black carbon (BC) at 4.4 days. Several studies examined the lifetime of BC in AeroCom Phase I and other models, ranging from 3.3 to 11.4 days (Bond et al., 2013; Koch et al., 2009; Schulz et al., 2006). Several studies suggested that BC lifetime should be shorter than 4–5 days, based on model comparisons with HIPPO (HIAPER Pole-to-Pole Observations; Schwarz et al., 2017) measurements, the first set of BC observations over the remote ocean (Bauer et al., 2013; Samset et al., 2014; Q. Wang et al., 2014; X. Wang, Heald, et al., 2014).

Discrepancies between the modeled aerosol lifetime among different models led to further discussions on the governing processes. Yu et al. (2019) suggest that the convective scheme in the CESM model transports aerosol into the upper troposphere too efficiently, extending BC lifetime, and producing an overestimation of BC mass concentrations. While some studies have found that wet scavenging plays a crucial role in the lifetime of aerosols. For instance, Q. Wang et al. (2014) modified the wet scavenging scheme in the GEOS-Chem model to better match HIPPO observations; however, the median concentration remained biased high by a factor of 2. Using the same HIPPO observations, X. Wang, Heald, et al. (2014) decreased the simulated lifetime of BC by increasing the rate of aging from hydrophobic to hydrophilic aerosol and therefore the solubility of BC. Modifying the wet deposition process in CAM5, H. Wang et al. (2013) found stronger BC removal and a better simulated seasonal cycle. Bian et al. (2017) found wet deposition to be the main factor in nitrate and ammonium lifetime diversity between models.

Wet scavenging removes particles by precipitation and is generally more effective than dry deposition for fine aerosols (Textor et al., 2006). Despite the central importance of wet processes for controlling the mass load and redistribution of aerosols, this process is not well-constrained, and new efforts in recent studies have modified the representation of wet scavenging processes (Liu & Matsui, 2021; Shan et al., 2021; H. Wang et al., 2013; Yu et al., 2019). Models typically include rainout (in-cloud) and washout (below-cloud) as two mechanisms of wet scavenging; rainout loss is often parameterized as a first-order function of constant in-cloud condensed water (Giorgi & Chameides, 1986). There are limited observational constraints available to test this representation, particularly far from sources. Since inorganic aerosols concentrations are often overestimated in models (Bian et al., 2017; Heald et al., 2012; Nault et al., 2021; Pye et al., 2009; Walker et al., 2012; Zakoura & Pandis, 2018; L. Zhang et al., 2012), recent work by Luo et al. (2019; 2020) revised the existing representation of wet processes in the GEOS-Chem global chemical transport model.

The wide range of aerosol lifetime estimates in model comparison studies, as well as the suggestion of a shorter BC lifetime from HIPPO, highlight the importance of investigating aerosol lifetime using similar remote globally distributed observations for all aerosols. Previous chemical transport modeling comparisons against ground and aircraft observations focus primarily over or near continental regions. For these campaigns, aerosols are generally sampled within a few days of being emitted or formed; thus, they are often a good constraint on emission and formation processes. In addition, most studies focus on a single or a subset of fine aerosol species (e.g., BC, Q. Wang et al., 2014; X. Wang, Heald, et al., 2014; OA, Chung & Seinfeld, 2002; Heald et al., 2005, 2006, 2011;

Hodzic et al., 2009; and inorganic aerosols, Adams et al., 1999; Heald et al., 2012; Park et al., 2004]. The NASA Atmospheric Tomography Mission (ATom), which surveyed the remote atmosphere from nearly pole-to-pole over the Atlantic and Pacific Oceans, offers us a first comprehensive data set of the remote atmosphere for all four seasons (Wofsy et al., 2018). By exploring the whole suite of fine aerosols, OA, BC, sulfate, nitrate, and ammonium, this campaign provides a comprehensive picture of aerosol abundance and distribution as well as new insights into the spatial (Northern [NH] and Southern Hemispheres [SH], Atlantic, and Pacific Oceans) and temporal (all seasons) variability in aerosol composition, separated from near-field source influences.

In this paper, we evaluate fine aerosols simulated by the standard GEOS-Chem transport model against aircraft observations from the ATom mission. This is the first study to report a suite of simulated fine aerosol lifetimes from a model, based on concentrations evaluated against observations in the remote atmosphere.

2. Model Description

We use the GEOS-Chem global chemical transport model (www.geos-chem.org) version 12.1.1 (https://doi.org/10.5281/zenodo.2249246) to simulate fine aerosols in this study. The simulations have a spin-up time of 6 months, with a chemical timestep of 20 min and a transport timestep of 10 min, as recommended by Philip et al. (2016). The simulations are performed with a $2° \times 2.5°$ horizontal resolution from the surface to the lower stratosphere in 47 vertical levels. The meteorology is driven by the Modern-Era Retrospective analysis for Research and Applications (MERRA-2) from the Goddard Earth Observing System (GEOS) of the NASA Global Modeling and Assimilation Office (Bey et al., 2001). Model simulations are performed for all four deployments of the ATom campaign (from 2016 to 2018) with the model sampled along the flight tracks.

The chemistry in GEOS-Chem includes SO_4^{2-}-NO_3^--NH_4^+ thermodynamics using the ISORROPIA II model (Fountoukis & Nenes, 2007), which has been evaluated against measurements and performs well for the partitioning (Cheng et al., 2021; Guo et al., 2018; Nah et al., 2018), coupled to a HO_x-NO_x-VOC-O_3 chemical mechanism (Mao et al., 2013; Miller et al., 2017; Travis et al., 2016) with integrated Cl-Br-I chemistry (Sherwen et al., 2016). The model simulates sulfate-nitrate-ammonium aerosol (Park, 2004; Pye et al., 2009), BC (Park et al., 2003), sea-salt (Jaeglé et al., 2011), and mineral dust (Fairlie et al., 2007; Ridley et al., 2012) using a bulk aerosol scheme with fixed log-normal modes (Martin et al., 2003). The simulation includes hydrophilic (BCPI) and hydrophobic (BCPO) black carbon, as well as oxygenated organic aerosol (OPOA) and emitted organic aerosol (EPOA), which represent hydrophilic and hydrophobic OA. BC and OA are emitted as 80% and 30%–50% hydrophobic, respectively (Park et al., 2004). We also adopt the conventionally used organic aerosol to organic carbon (OA:OC) ratio in our OA calculations, 1.4 for the fresh EPOA and 2.1 for the aged OPOA. GEOS-Chem employs two SOA schemes of different levels of complexity and mechanistic representation, commonly referred to as the "complex scheme" and the "simple scheme." The former includes an explicit chemical mechanism for the oxidation of isoprene. POA is treated as semi-volatile, and SOA formation is modeled based on the volatility-basis set (Marais et al., 2016; Pye & Seinfeld, 2010); whereas, the latter offers a simple alternative that provides computational efficiency by neglecting mechanistic representation of the SOA evolution as well as partitioning by treating all OA as nonvolatile (Chin et al., 2002; Cooke et al., 1999). A comprehensive description and an evaluation of the two schemes against a suite of aircraft observations are detailed in Pai et al. (2020), and as noted by the authors, the simple scheme is not a simplified version of the complex scheme. We verify that, consistent with Pai et al. (2020), there is no significant difference in the total simulated OA mass concentrations during ATom using these two schemes. Since the complex scheme is the state-of-the-art OA scheme in GEOS-Chem and provides greater detail for OA speciation, we use the complex scheme for this study. In the complex scheme, OA is speciated by their type: the anthropogenic SOA from light aromatic oxidation (ASOA), the terpene SOA from monoterpene and sesquiterpenes oxidation (TSOA), and isoprene SOA (ISOA) consisting of aerosol-phase glyoxal, isoprene epoxydiols (IEPOX), C_4 epoxides, methylglyoxal, and low-volatility non-IEPOX products of isoprene hydroxy hydroperoxide oxidation, as well as various products from isoprene and monoterpene organo-nitrates oxidation pathways (OrgNit) whose components are split into OAs and nitrate for the comparisons shown here. GEOS-Chem also assumes externally mixed aerosols with fixed log-normal size distribution (Martin et al., 2003).

Emissions are configured using the Harvard-NASA Emissions Component (HEMCO; Keller et al., 2014), where global anthropogenic emissions are taken from the Community Emissions Data System (CEDS) v2018-08 inventory (Hoesly et al., 2018). Regional inventories, for instance, the Big Bend Regional Aerosol and Visibility Observational (BRAVO) inventory for Mexico (Kuhns et al., 2005), the Criteria Air Contaminants

(CAC) inventory for Canada, the Diffuse and Inefficient Combustion Emissions (DICE) inventory for Africa (Marais & Wiedinmyer, 2016), the European Monitoring and Evaluation Program (EMEP) inventory for Europe, the National Emissions Inventory (NEI 2011) for the United States, and the MIX inventory Asian emissions (Li et al., 2017), override emissions from CEDS. Monthly biomass burning emissions are from the Global Fire Emissions Database version 4 (GFED4; Giglio et al., 2013), and biogenic emissions are based on the Model of Emissions of Gases and Aerosols from Nature (MEGAN v2.1) emissions model (Guenther et al., 2012).

Removal processes in the model include dry and wet deposition. Gas and aerosol dry deposition use a resistor-in-series parameterization (Wesely, 1989; L. Zhang et al., 2001). Wet deposition includes in-cloud scavenging "rainout," whose first-order parameterization and loss rate are based on Giorgi and Chameides (1986), and below-cloud scavenging "washout" (Amos et al., 2012; Jacob et al., 2000; H. Liu et al., 2001). Recent updates in the wet scavenging scheme in GEOS-Chem by Luo et al. (2019) reduce biases in simulated nitric acid, nitrate, and ammonium. Since studies have shown great difference between modeled and size-resolved washout rates (Andronache et al., 2006; Henzing et al., 2006; Laakso et al., 2003; X. Wang et al., 2010). The aerosol wet removal parameterization in GEOS-Chem consists of scavenging in convective updrafts and rainout and washout by precipitation (H. Liu et al., 2001). For scavenging in convective updrafts due to vertical transport, a fraction of aerosols in air (α dz) is lost when the air is lifted up a distance of dz, where α is the scavenging efficiency. For a column of updraft air with a thickness of Δz, the scavenged aerosol fraction f is calculated as $f = 1 - e^{-\alpha\Delta z}$.

For the rainout by precipitation, the rainout water-soluble species are originally parameterized in GEOS-Chem as:

$$F = \frac{P_r}{k \cdot \text{ICCW}} \left(1 - e^{-k \cdot \Delta t}\right)$$

where F is the fraction of a water-soluble tracer in the grid box scavenged by rainout, Δt is the model integration time step, and k is the first-order rainout loss rate (Giorgi & Chameides, 1986), ICCW is the in-cloud condensation water, and P_r is the rate of new precipitation formation (rain only) in the corresponding grid box.

The new scheme (Luo et al., 2019) replaced the previously assumed constant ICCW, as the authors found that fixed ICCW value led to overestimations of nitrate and ammonium mass concentration. The new scheme calculates F using time and location-dependent ICCW from the MERRA-2 meteorological fields, and considers P_r not as a grid-box mean value anymore, but as an in-cloud value by including the cloud fraction, consistent with ICCW. The updated ICCW is calculated as:

$$\text{ICCW} = \frac{\text{LCW} + \text{ICW} + P_r \cdot \Delta t}{f_c}$$

where f_c is the grid-box mean cloud fraction, LCW is the liquid-phase cloud water content, and ICW is the ice-phase cloud water content. The updated rainout loss fraction becomes:

$$F = \frac{f_c \cdot P_r}{k \cdot (\text{LCW} + \text{ICW} + P_r \cdot \Delta t)} \left(1 - e^{-k \cdot \Delta t}\right)$$

The rainout efficiency for water-soluble aerosols is set to be 100% in GEOS-Chem. In a subsequent study, Luo et al. (2020) further developed the scheme by updating rainout efficiencies for carbonaceous aerosols, as follows:

$$F = \frac{f_c \cdot P_r}{k \cdot (\text{LCW} + \text{ICW} + P_r \cdot \Delta t)} \left(1 - e^{-E_r \cdot k \cdot \Delta t}\right)$$

where E_r is the rainout efficiency for corresponding species. We have summarized the rainout efficiencies for the carbonaceous aerosols in Table S1 in Supporting Information S2.

For washout by precipitation, the model uses a constant washout rate, which is applied to the precipitating fraction of the grid square, and the aerosol washout fraction is calculated by:

$$F_{\text{wash}} = f_r \left(1 - \exp\left(-k_{\text{wash}}\Delta t\right)\right)$$

where f_r is the horizontal fraction of the precipitating area in the grid box, and k_{wash} is the washout rate, which is calculated using:

$$k_{\text{wash}} = \Lambda \left(\frac{P_{\text{r}}}{f_{\text{r}}} \right)^{b}$$

where Λ is the washout scavenging coefficient, and b is an exponential coefficient, both of which are treated as constants (Q. Wang et al., 2011). For the updated scheme, Luo et al. (2019, 2020), adopt species-specific scavenging coefficients (Λ and b) based on field measurements (Laakso et al., 2003; X. Wang, Zhang, et al., 2014). These Λ and b values for aerosol washout rates by rain and snow are summarized in table 1 of Luo et al. (2020).

Shan et al. (2021), which used CESM2 CAM6, highlighted the main wet deposition parameters: aerosol activation, removal, and resuspension rates. We note here that aside from the removal rate determined by the rainout equation above, the model assumes its bulk aerosols are in the accumulation mode and are easily activated into cloud droplets. Therefore, their activation rate is assumed to be 100%. For resuspension, the model assumes 100% of the aerosols in rainwater would return to the atmosphere when resuspension takes place. The resuspension rate is calculated using $R = 0.5 * \frac{L_{\text{top}} - L_{\text{bottom}}}{L_{\text{top}}}$, where R is the resuspension rate, L_{top} is the rainwater from the layer top, and L_{bottom} is the rainwater from the layer bottom; this gives the range of resuspension rate to be $0 \leq R \leq 0.5$. Please note that in this study, we first use the model's standard wet deposition scheme, then in Section 4.1, we explore the impact of using the updated wet deposition scheme from Luo et al. (2019).

3. ATom Observations

The ATom campaign (Wofsy et al., 2018) surveyed global cross-sections of aerosol composition in the remote troposphere, while flying near-continuous ascents and descents and profiling the atmosphere over 0.15–12.7 km over the Pacific and Atlantic Oceans from approximately 80°N to approximately 65°S (Brock et al., 2019); flight tracks are shown in Figure 1. This measurement scheme provides unbiased sampling, ideal for model validation on a global scale (Strode et al., 2015). The Aerodyne High-Resolution Time-of-Flight Aerosol Mass Spectrometer (AMS, Canagaratna et al., 2007; DeCarlo et al., 2006; Jimenez et al., 2019) is used to measure non-refractory submicron PM1 species in this study: OA, sulfate, nitrate, and ammonium; the Single Particle Soot Photometer (SP2; Katich et al., 2018) is used to capture the accumulation-mode refractory BC aerosol. Both the AMS and SP data are merged as 10 s mean. Details for the operation of the AMS can be found elsewhere (Guo et al., 2021; Nault et al., 2018; Schroder et al., 2018). Though the detection limits for OA, sulfate, nitrate, and ammonium can vary by region (Hodzic et al., 2020), they generally are on order 0.1, 0.015, 0.015, and 0.005 µg/sm^3, respectively (Guo et al., 2021). The accuracy of the AMS mass concentration is 35% (sulfate, nitrate, and ammonium) and 38% (OA) (Bahreini et al., 2009; Guo et al., 2021). For most of ATom, the AMS quantified particles between 20 and 770 nm geometric diameter, fully capturing the accumulation mode and most of the Aitken mode in the remote troposphere (Brock et al., 2019; Guo et al., 2021; Williamson et al., 2019). Aerosol mass concentrations are reported at conditions of standard temperature and pressure (STP: $T = 273K$, $P = 1$ atm) in µg/sm^3; note that model concentrations are also shown at STP. The ATom dataset includes four surveys in July–August 2016 (ATom-1, NH summer), January–February 2017 (ATom-2, NH winter), September–October 2017 (ATom-3, NH fall), and April–May 2018 (ATom-4, NH spring). We use a land mask to filter the data set and only examine measurements over the oceans, representative of aged or remote conditions, and we only use data below the dynamic tropopause height to remove observations in the stratosphere. We also filter out concentrations above the 97th percentile from every species in the data set to eliminate the impact of any plumes that cannot be captured by Eulerian models (Rastigejev et al., 2010); we note that this includes some biomass burning plumes sampled off of Africa. We include measurements reported below the detection limit in our analysis to avoid biasing mean values; as discussed by Hodzic et al. (2020).
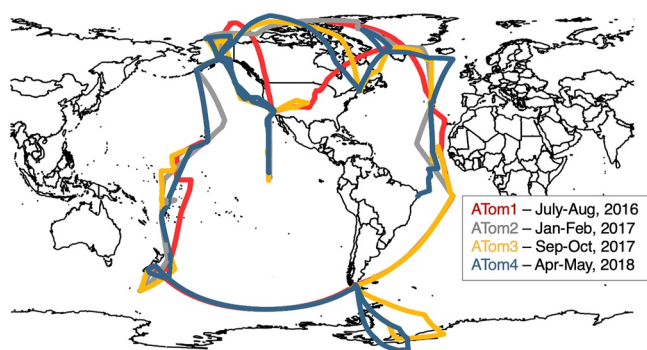

Figure 1. Flight tracks for the four deployments of the ATom field campaign.
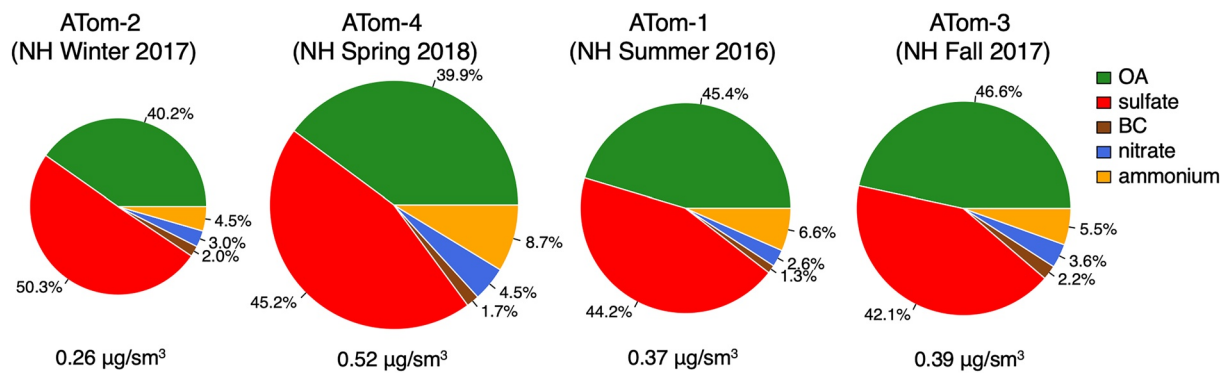
Figure 2. Mean aerosol mass concentrations observed during each ATom survey (proportional to the area of each pie and listed at the bottom). Pie charts show the relative contribution of each species. Each deployment is labeled with the corresponding season in the Northern Hemisphere.

4. Results

4.1. Mass Concentration of Remote Atmospheric Aerosols

The mean observed concentrations of remote OA, BC, sulfate, nitrate, and ammonium aerosols during ATom vary by season (Figure 2, we note that all seasonal labels herein follow NH designations); summer and fall have similar mean total concentrations at 0.37 and 0.39 μg/sm^3, whereas winter is cleaner at 0.26 μg/sm^3, and spring is more polluted at 0.52 μg/sm^3. Fine aerosol species concentrations are dominated by OA and sulfate in all deployments, making up more than 85% of the total aerosol concentration, with more OA present in summer and fall, and more sulfate in winter and spring. The fractional contribution of BC, nitrate, and ammonium show less variation across seasons, though mass concentrations of all peak in the spring. Comparing concentrations in NH and SH (Figure S1 in Supporting Information S1), the greatest difference is evident in ATom-4 (spring in the NH), where mean total aerosol concentrations are about twice as high in the NH than in the SH (0.61 and 0.3 μg/sm^3 respectively), and the sulfate to OA ratio is about twice as high in the SH (1:1 and 2:1 in the North and South, respectively). To estimate source contributions, we turn off anthropogenic and biomass burning emissions in turn and difference these with the baseline simulation. Figure 3 shows that while anthropogenic sources contribute the majority of the simulated BC, nitrate, and ammonium sampled during the ATom deployments in all seasons, OA and sulfate, the two dominant species, have important non-anthropogenic sources (i.e., biogenic SOA, and natural sulfate from dimethyl sulfide oxidation).

Figure 4 compares the observed and simulated vertical distribution of aerosol mass concentrations of the five species for each ATom survey. The normalized mean bias, for which a positive number indicates that the model result is biased high, is listed as NMB on each of the subplots. Simulated mass concentrations reproduce the vertical profile of the measurements, but are generally biased high, which is consistent with most other state-of-the-art global models (Hodzic et al., 2020; Pai et al., 2020; Tilmes et al., 2019). This bias is most evident across all species in ATom-2 (NH winter). Lower tropospheric concentrations are also biased high in ATom-4 (NH spring) for all species except nitrate. Biases are more modest in ATom-1 (NH summer) and ATom-3 (NH fall). The model captures the vertical structure best for BC and sulfate ($R^2 = 0.45–0.95$) and worst for nitrate ($R^2 = 0.26–0.78$).

The bias during ATom-2 (NH winter) is dominated by aerosol in the North Pacific (shown in Figure 5 for OA and sulfate). Pai et al. (2020) also identified this model overestimate of the OA concentrations in ATom-2 and suggested that it was driven by anthropogenic organics in the North Pacific. Spatial cross-sections of all simulated species mass concentration at 4 km, at which height the bias is most significant for NH winter (ATom-2), exhibit prominent Asian outflow for all five aerosols over the North Pacific Basin (Figure S2 in Supporting Information S1). This is consistent with previous aircraft observations studies that identify transpacific transport of aerosols over the Pacific (Andreae et al., 1988; Arimoto et al., 1997; Clarke et al., 2001; Heald et al., 2006; Jordan et al., 2003; Maxwell-Meier et al., 2004; Price et al., 2003). Similarly, the NH spring (ATom-4) sulfate high bias in the lower troposphere is most prominent in the North Pacific, which is consistent with the springtime peak in intercontinental transport of aerosol from Asia (e.g., Heald et al., 2006). In addition, Figure S3 in Supporting Information S1 confirms that anthropogenic sources contribute the majority of all the simulated species during ATom-2 in the North Pacific, where the Asian outflow takes place.
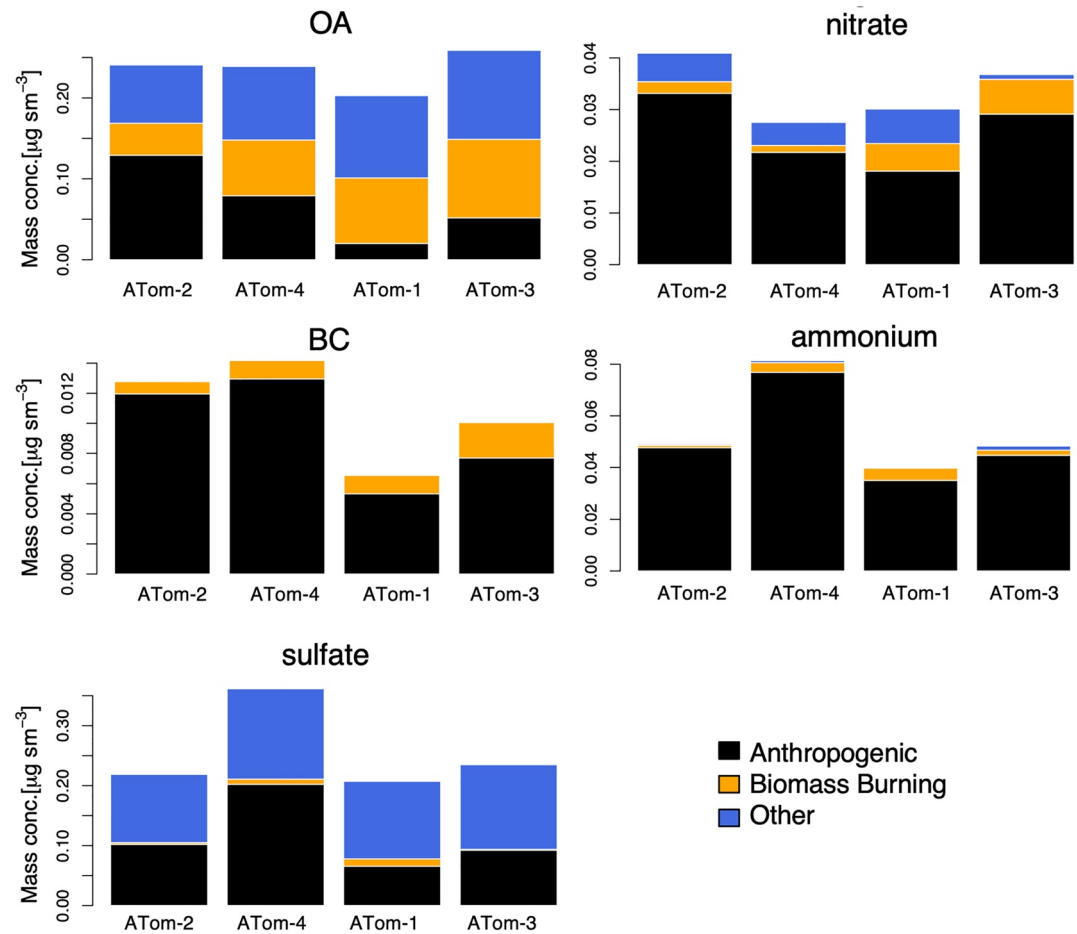
Figure 3. Emission source contribution (anthropogenic in black, biomass burning in orange, and other sources in blue) to the simulated mass concentrations along the ATom flight tracks during each deployment in the North Pacific. Other here includes aerosol precursors such as DMS, natural sources of NOx, and biogenic VOCs.

We perform an idealized sensitivity test to confirm that the concentrations are sensitive to Asian emissions in winter. Figure 6 shows the comparison when we reduce Asian anthropogenic emissions from the MIX inventory by half. This emission reduction improves the simulations but does not entirely eliminate the high bias. Therefore, further Asian anthropogenic emissions reductions to resolve this bias would be unrealistic.

Since source biases are unlikely to explain the bias across species observed during ATom-2, we consider the role of aerosol removal. We find that with Luo et al. (2019)'s updates, wet removal generally decreases over the tropics and increases poleward. The top row of Figure 4 shows how the updated wet scavenging scheme improves the model simulation for ATom-2 (shown as thin colored lines). The high bias is almost entirely eliminated across all species (see improvement in NMB); furthermore, the shape of the vertical profiles and the aerosol concentration magnitudes are well captured by the model with these updates, with particularly significant improvements in the R^2 for nitrate and ammonium. We have also included the ATom-2 OA and sulfate profiles for each basin in Figure S4 in Supporting Information S1, which also compare better comparison and are consistent with results of overall totals for each aerosol shown in Figure 4. The effects of these updates are shown for all seasons in the subsequent rows of Figure 4. The impact of these wet scavenging updates is smaller for the ATom-1 and ATom-3 simulations (which were previously less biased), but also generally improves the comparison with observations (both in terms of a reduction in NMB and a general, though not universal, increase in R^2). However, for ATom-4 (NH spring), the wet scavenging updates appear to excessively remove aerosol particularly aloft, leading to a low bias. This could suggest the need for additional sources from Asia in this season, or alternatively, biases in the removal efficiency in this season; further investigation is needed, for instance, the newly adapted rates need further investigation, as noted in Luo et al. (2019), the difference in empirical washout rates from theoretical and
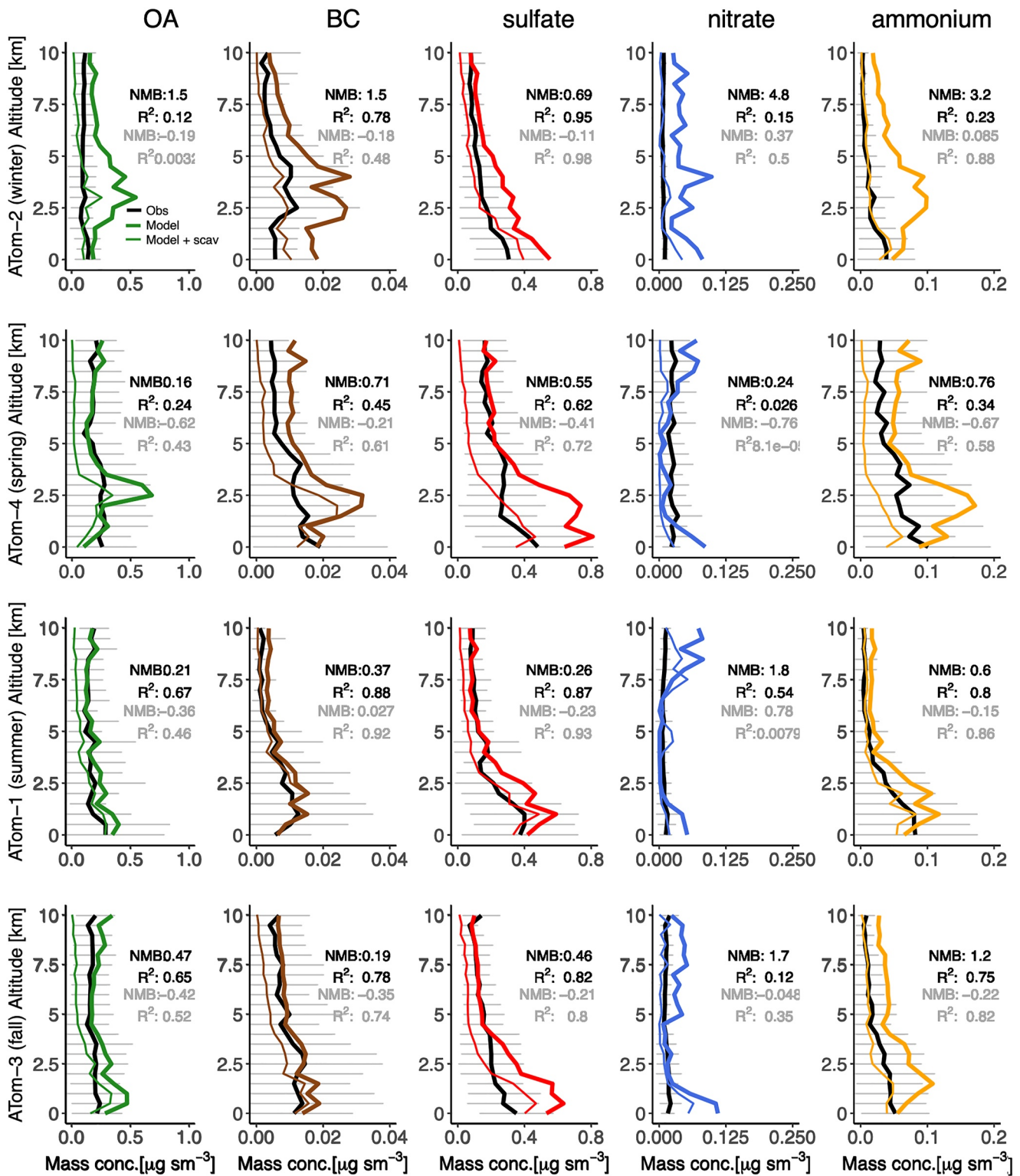
Figure 4. Mean vertical profiles of aerosol mass concentration as simulated with the standard GEOS-Chem model (thick colored lines) and observed (black, standard deviation shown in gray) during the ATom campaign for all four deployments (season in reference to Northern Hemisphere [NH]): ATom-1 (NH summer 2016), ATom-2 (NH winter 2017), ATom-3 (NH fall 2017), and ATom-4 (NH spring 2018). The normalized mean bias (NMB) and R^2 of the comparison are shown inset in each panel. Also shown are the concentrations simulated with updated wet scavenging ("Model + scav"; thin colored lines), and the associated NMB and R^2 in gray text.
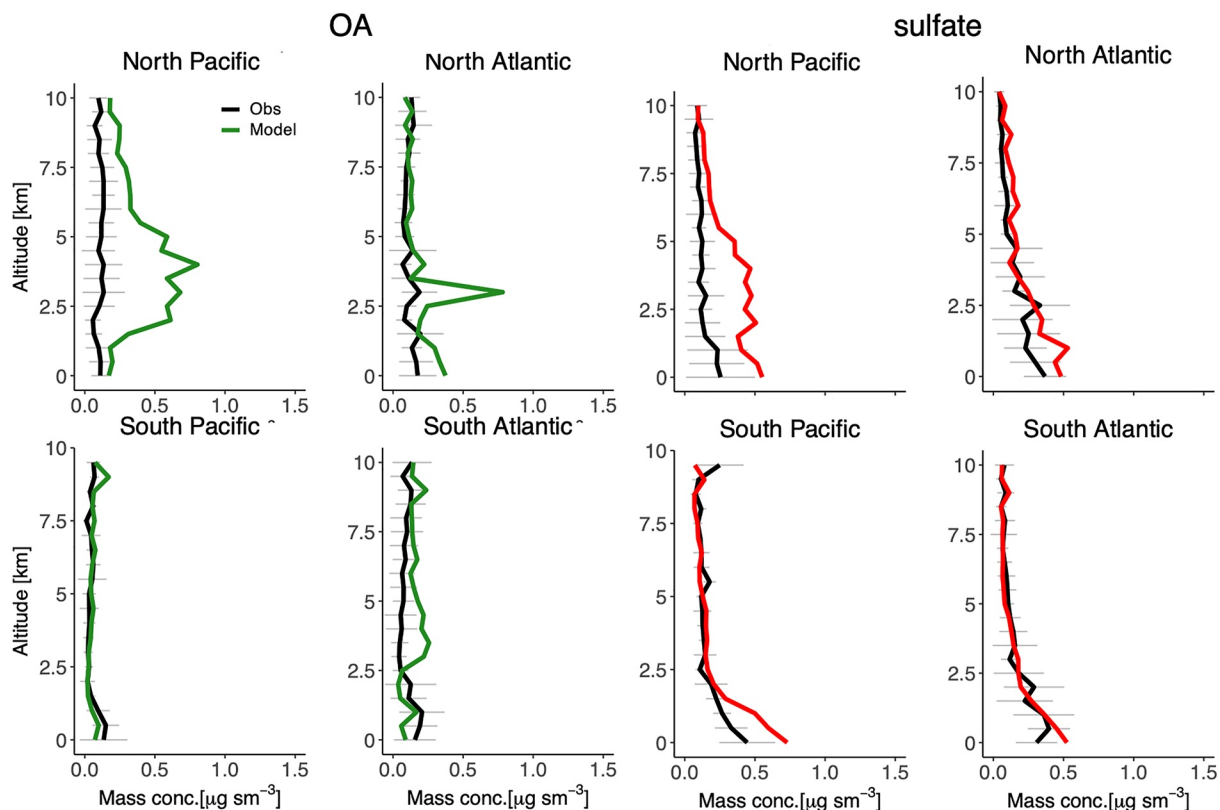
Figure 5. Vertical profiles of mean mass concentration simulated with GEOS-Chem (organic aerosol in green, sulfate in red) and observed (black) during ATom-2 (NH winter 2017) deployment divided into ocean basins (Northern Hemisphere is defined as 0–90°N, Southern Hemisphere is defined as 0–90°S). Standard deviation shown in gray.

field studies remain large. We highlight here the significant sensitivity of remote aerosol concentrations to the parameterization of wet removal.

4.2. Organic Aerosols

Given the importance of OA during ATom and the complexity of this source of aerosol, here we expand our investigation of this species. Note that from this point, all simulations include the updated wet scavenging scheme.
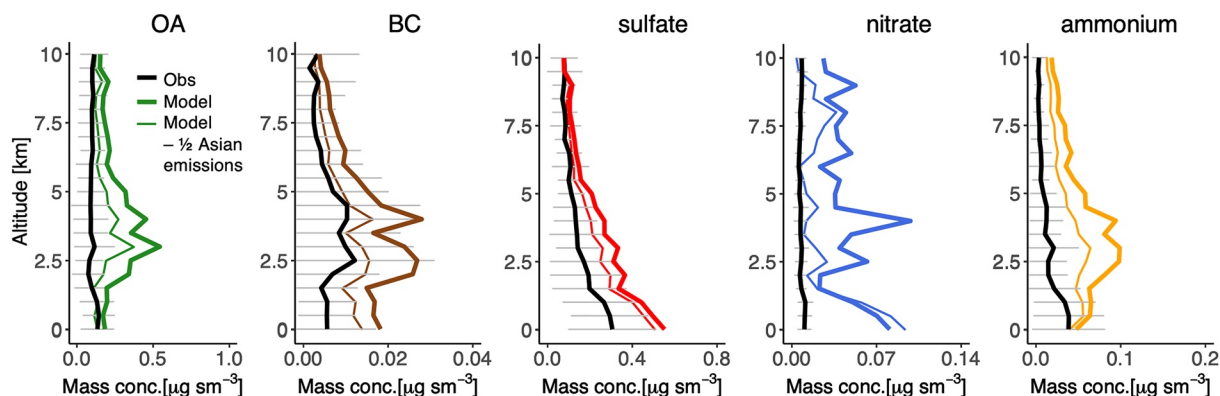

Figure 6. Mean vertical profiles of aerosol mass concentrations observed (black lines) and simulated with GEOS-Chem (thick colored lines) ATom-2 (NH winter) (standard deviation in gray). Results from the sensitivity simulation where anthropogenic emissions from Asia have been decreased by half are shown as thin colored lines.
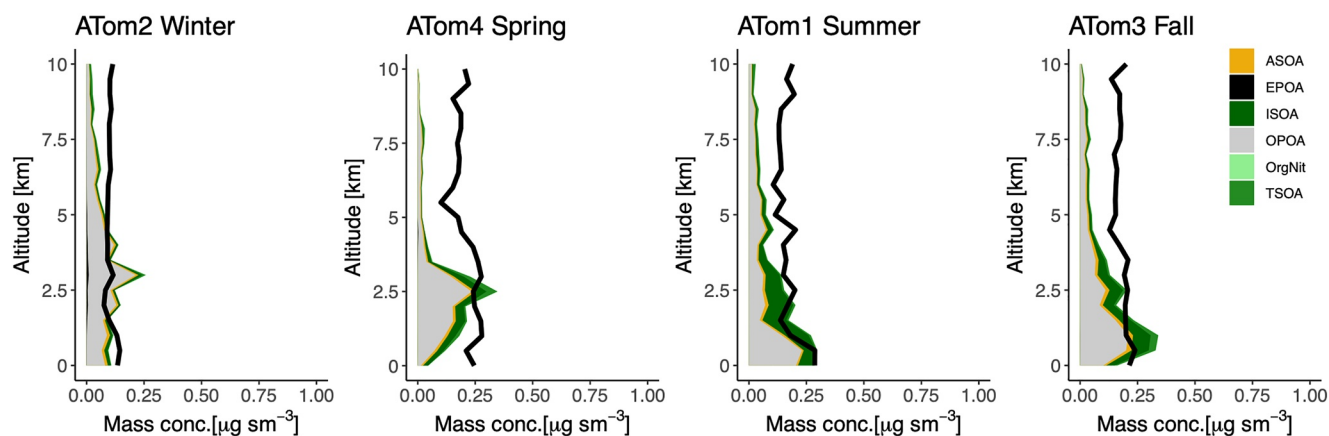
Figure 7. Mean vertical profiles of organic aerosol mass concentrations observed (black lines) and simulated with GEOS-Chem (colored sections show various contributions) for all four ATom deployments. Here simulations include the wet scavenging update. ASOA is anthropogenic SOA from light aromatic oxidation, EPOA is freshly emitted organic aerosol, OPOA is oxygenated organic aerosol, OrgNit is the organic portion of the organo-nitrates from isoprene and monoterpene, ISOA is aerosol-phase glyoxal, isoprene epoxydiols (IEPOX), C_4 epoxides, methylglyoxal, and low-volatility non-IEPOX products of isoprene hydroxy hydroperoxide oxidation, and TSOA is terpene SOA from monoterpene and sesquiterpenes oxidation.

Figure 7 shows that, with the emission inventories used in this study, the oxygenated OPOA dominates (>50%) total OA mass concentration, given that freshly emitted EPOA from anthropogenic and biomass burning sources age during transport to remote regions. EPOA is only present in winter (ATom-2), indicative of a small amount (<5%) of fresh OA. This EPOA is also only present in the North Pacific, consistent with higher wind speeds and faster intercontinental transport from Asia to North America (i.e., less aging).

The OA:OC ratio indicates the degree of organic carbon oxidation and increases with the chemical aging of OA; previous studies suggest a range of 1.2–2.5 (Aiken et al., 2008; Grosjean & Friedlander, 1975; Heald et al., 2010; Malm et al., 1994; Pang et al., 2006; Philip et al., 2014; Turpin & Lim, 2001; White & Roberts, 1977; Q. Zhang et al., 2005). ATom measurements represent some of the most aged air masses sampled by aircraft, and thus have a higher OA:OC ratio. Hodzic et al. (2020) show that values range from ~1.5 to 3.5, with an average of 2.4 during ATom-1 and ATom-2. Since we find that EPOA makes a negligible contribution to air masses sampled during ATom, the OA:OC assumed for this component does not impact our comparisons. The OA:OC applied to OPOA in the model is 2.1, only marginally smaller than the average observed during ATom; increasing to 2.4 has a modest (~15%) impact on the comparison of means shown in Figure 7. The ATom measurements clearly indicate that a spatially and/or temporally dynamic representation of OA:OC is needed to capture the observed range of aging; however, additional measurements constraining the evolution of OA:OC in continental export are needed to parameterize this process.

Figure 7 shows that upon updating our wet scavenging scheme, our model simulation of free tropospheric concentrations of OA are biased low, particularly in well-aged air masses aloft. This bias is systematic, that is, not limited to one particular basin or latitude (Figure S4 in Supporting Information S1). Implementing photochemical loss, as previously described by Hodzic et al. (2015, 2016) to the standard and updated model both produced extremely low OA concentrations; in winter completely zero'ing out OA. Photolysis loss is expected to peak in local summer; however, we find our model biases are at a minimum in this season (Figure 7). Recent laboratory experiments find that for some species, the loss rate of OA by photolysis slows significantly after an initial decline and plateaus, suggesting the existence of a non-photolabile fraction (O'Brien & Kroll, 2019; Zawadowicz et al., 2020). Considering the large impact of wet scavenging changes on simulated OA, as well as the lack of seasonal support and recent laboratory constraints on the photochemical sink, it seems unlikely that photochemical loss is a dominant process for controlling remote aerosol lifetime, but rather that additional work on OA scavenging parameters is needed.

4.3. Lifetime of Aerosols

Aerosols in GEOS-Chem have been extensively explored and validated over continental regions (e.g., Leibensperger et al., 2012; Pai et al., 2020; Pye et al., 2009; X. Wang, Heald, et al., 2014], which gives us

Table 1
Annual (2017) Simulated Aerosol Budget With Wet Scavenging Updates

Species	Burden (Tg)	Loss (Tg/yr)	Dry dep. (Tg/yr)	Wet dep. (Tg/yr)	Lifetime (days)
OA	1.4	128.6	13.9	114.4	4.0
BC	0.1	8.9	1.5	7.4	4.0
Sulfate	0.8	140.8	11.8	129.0	2.1
Nitrate	0.1	17.1	3.2	13.9	3.1
Ammonium	0.2	38.2	3.0	35.3	1.9

confidence that the model generally captures near-field aerosol emissions and formation magnitudes (We note here that the GEOS-Chem model resolution does not resolve the very near-field (i.e., urban to sub-urban) evolution). However, aerosol lifetime which ultimately controls global aerosol abundance, is rarely diagnosed in models.

Table 1 summarizes the annual mean simulated global burden, loss separated by dry and wet deposition, and lifetime for the five aerosol species in the simulation year 2017, including the wet deposition updates. OA has the highest global burden at 1.4 Tg, and sulfate follows at 0.8 Tg. For all the species, wet deposition is more effective than dry deposition, contributing more than 80% of the loss. Aerosol lifetime ranges from 1.9 to 4 days, with carbonaceous aerosol having the longest lifetimes at 4 days, consistent with an initial hydrophobic fraction.

The aerosol lifetimes simulated with the updated wet scavenging are shorter than those found in previous studies (discussed in Section 1). The mean annual lifetime of BC is 4 days, which aligns with suggestions by Bauer et al. (2013) and Samset et al. (2014) that BC lifetime should be on the lower end of those simulated in current models (3.8–17.1 days), but shorter than the average of 5.5 days from Gliβ et al. (2021). The average lifetime of 4.0 days for OA is on the lower end of a mean of 5.7 (±1.6 days) found in the AeroCom Phase II ensemble models (Tsigaridis et al., 2014). The lifetimes of the inorganic aerosols are also on the lower end of those simulated in the AeroCom Phase III models summarized by Bian et al. (2017) and Gliβ et al. (2021).

Figure 8 demonstrates that the aerosol lifetime is very sensitive to the wet removal scheme. Without the wet scavenging updates, the annual mean lifetimes of OA, sulfate, and ammonium are ~2 days longer, and the BC and nitrate lifetimes are ~1 day longer (see Table S2 in Supporting Information S2). There is little seasonal variation in global mean lifetime, with no more than half a day variation for each species across the seasons. However, as expected, the seasonal variability is more pronounced in each hemisphere, particularly for carbonaceous aerosol (Figure S5 in Supporting Information S1). Carbonaceous aerosol lifetimes are shortest during local summer and fall in each hemisphere; likely due to a combination of faster photochemical processing of SOA, increased precipitation, and changing transport. The longest aerosol lifetimes (5–6 days) are for carbonaceous aerosol in the SH during the fire season (July–November).

As shown in Section 4.1, the wet scavenging updates bring our simulated aerosol mass concentration into good agreement with observed concentrations in the NH winter as well as NH summer and NH fall, suggesting that such decreases in lifetime are necessary. However, as noted, the updates also led to excessive removal in the NH spring (Figure 4), suggesting that the simulated aerosol lifetime in April-May may be underestimated. Similarly, the underestimates in OA aloft shown in Section 4.2 may indicate that the OA lifetimes are too short throughout
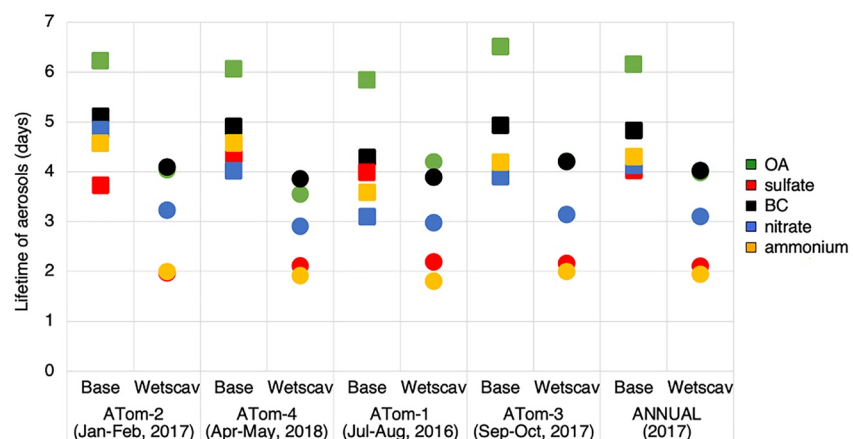

Figure 8. Global mean seasonal and annual lifetime of the five aerosols in the base simulation and the updated wet scavenging simulation.

the year. These comparisons highlight the need for further study of the aerosol removal process, and the sensitivity to precipitation processes.

5. Conclusions

The ATom measurements offer a first look at aerosol abundance and composition in the global remote atmosphere across seasons. Seasonal mean total aerosol concentrations range from 0.26 to 0.52 μg/sm^3, with ATom-2 (NH winter) being the cleanest and ATom-4 (NH spring) the most polluted. Aerosol composition is dominated by OA and sulfate in all seasons, and the former has a higher fraction in the NH summer and NH fall, whereas the latter has a higher fraction in the winter and spring. Comparisons of simulated and observed aerosol concentrations during the ATom-2 campaign show a systematic NH winter high bias for all aerosols. Wet scavenging updates in the model by Luo et al. (2019, 2020) eliminate the bias during ATom-2; however, the new scheme appears to excessively remove aerosol during ATom-4 (NH spring) and underestimate OA aloft. The updated simulation otherwise captures the vertical distribution, magnitude, and composition of remote aerosols observed during ATom.

We show that anthropogenic, biomass burning, and biogenic sources all contribute about equally to mean simulated remote OA concentrations, with important seasonal variations between ATom deployments. We find that, including photolysis, loss produces extremely low to zero OA concentrations in the model. Finally, we note that while the large variability in observed OA oxidation level (OA:OC) is unlikely to substantially impact our comparison of mean concentrations, it strongly supports the need to develop a dynamic OA aging scheme to better constrain and represent the OA evolution from continental to remote regions, as also noted by Hodzic et al. (2020).

Wet removal processes determine the magnitude of the aerosol lifetime in GEOS-Chem. Our results show that the aerosol lifetime is very sensitive to the updates in the wet scavenging scheme, which reduces the lifetime of all aerosols by 1–2 days. Given that concentrations generally compare well against ATom, the first such extensive remote data set, after these updates, our comparisons suggest that the lifetime of aerosols may have been overestimated by previous versions of GEOS-Chem and other similar models. Quantifying the impact of a 1–2 days overestimation of aerosol lifetime on climate is not possible with the model configuration used here. Qualitatively, shorter aerosol lifetime would reduce aerosol abundance in the atmosphere as well as long-range transport (Gliβ et al., 2021). Lower aerosol concentrations would therefore likely decrease aerosols' direct and indirect effects on climate; this should be explored in future work. At the same time, the substantial impact of these updates on the global aerosol lifetime suggests that more work is needed to constrain wet removal processes in models. For example, Y. Wang et al. (2021) suggest that excessive light rain in climate models leads to systematic underestimates of aerosol burden. Further evaluation of rain frequency in climate models and in assimilated meteorology is needed.

ATom offers unique insights into well-aged air masses in the remote atmosphere, which we exploit here to evaluate aerosol lifetime in a global model. However, we also note that, concentration comparisons alone are insufficient to indicate whether lifetime estimates are biased. For instance, a low bias in concentration could reflect an underestimate in the source, or an overestimate of the loss rate, for which the lifetime would also be biased. Also, further work is needed to better constrain the processes controlling aerosol lifetime. In particular, observations that track the export of aerosols from continental regions to the remote environment, alongside measurements of precursor species and cloud water content, could improve process-based understanding of removal mechanisms. Such measurements have the potential to help us better capture the aging process of aerosols, and in turn, their abundance and global impact.

Conflict of Interest

The authors declare no conflicts of interest relevant to this study.

Data Availability Statement

The GEOS-Chem model code is available at http://acmg.seas.harvard.edu/geos/, and the ATom: Merged Atmospheric Chemistry, Trace Gases, and Aerosols data can be accessed at https://doi.org/10.3334/ORNLDAAC/1581 (Wofsy et al., 2018).

References

Adams, P. J., Seinfeld, J. H., & Koch, D. M. (1999). Global concentrations of tropospheric sulfate, nitrate, and ammonium aerosol simulated in a general circulation model. *Journal of Geophysical Research: Atmospheres*, *104*(D11), 13791–13823. https://doi.org/10.1029/1999jd900083

Aiken, A. C., DeCarlo, P. F., Kroll, J. H., Worsnop, D. R., Huffman, J. A., Docherty, K. S., et al. (2008). O/C and OM/OC ratios of primary, secondary, and ambient organic aerosols with high-resolution time-of-flight aerosol mass spectrometry. *Environmental Science & Technology*, *42*(12), 4478–4485. https://doi.org/10.1021/es703009q

Amos, H. M., Jacob, D. J., Holmes, C. D., Fisher, J. A., Wang, Q., Yantosca, R. M., et al. (2012). Gas-particle partitioning of atmospheric Hg(II) and its effect on global mercury deposition. *Atmospheric Chemistry and Physics*, *12*(1), 591–603. https://doi.org/10.5194/acp-12-591-2012

Andreae, M. O., Berresheim, H., Andreae, T. W., Kritz, M. A., Bates, T. S., & Merrill, J. T. (1988). Vertical distribution of dimethylsulfide, sulfur dioxide, aerosol ions, and radon over the Northeast Pacific Ocean. *Journal of Atmospheric Chemistry*, *6*(1–2), 149–173. https://doi.org/10.1007/bf00048337

Andronache, C., Grönholm, T., Laakso, L., Phillips, V., & Venäläinen, A. (2006). Scavenging of ultrafine particles by rainfall at a boreal site: Observations and model estimations. *Atmospheric Chemistry and Physics*, *6*, 4739–4754. https://doi.org/10.5194/acp-6-4739-2006

Arimoto, R., Duce, R. A., Prospero, J. M., Savoie, D. L., Talbot, R. W., Dibb, J. E., et al. (1997). Comparisons of trace constituents from ground stations and the DC-8 aircraft during PEM-West B. *Journal of Geophysical Research*, *102*(D23), 28539–28550. https://doi.org/10.1029/97jd00192

Bahreini, R., Ervens, B., Middlebrook, A. M., Warneke, C., Gouw, J. A., DeCarlo, P. F., et al. (2009). Organic aerosol formation in urban and industrial plumes near Houston and Dallas, Texas. *Journal of Geophysical Research: Atmospheres*, *114*(D7), D00F16. https://doi.org/10.1029/2008jd011493

Balkanski, Y. J., Jacob, D. J., Gardner, G. M., Graustein, W. C., & Turekian, K. K. (1993). Transport and residence times of tropospheric aerosols inferred from a global three-dimensional simulation of 210Pb. *Journal of Geophysical Research: Atmospheres*, *98*(D11), 20573–20586. https://doi.org/10.1029/93jd02456

Bauer, S. E., Bausch, A., Nazarenko, L., Tsigaridis, K., Xu, B., Edwards, R., et al. (2013). Historical and future black carbon deposition on the three ice caps: Ice core measurements and model simulations from 1850 to 2100. *Journal of Geophysical Research: Atmospheres*, *118*(14), 7948–7961. https://doi.org/10.1002/jgrd.50612

Bey, I., Jacob, D. J., Yantosca, R. M., Logan, J. A., Field, B. D., Fiore, A. M., et al. (2001). Global modeling of tropospheric chemistry with assimilated meteorology: Model description and evaluation. *Journal of Geophysical Research: Atmospheres*, *106*(D19), 23073–23095. https://doi.org/10.1029/2001jd000807

Bian, H., Chin, M., Hauglustaine, D. A., Schulz, M., Myhre, G., Bauer, S. E., et al. (2017). Investigation of global particulate nitrate from the AeroCom phase III experiment. *Atmospheric Chemistry and Physics*, *17*(21), 12911–12940. https://doi.org/10.5194/acp-17-12911-2017

Bond, T. C., Doherty, S. J., Fahey, D. W., Forster, P. M., Berntsen, T., DeAngelo, B. J., et al. (2013). Bounding the role of black carbon in the climate system: A scientific assessment. *Journal of Geophysical Research: Atmospheres*, *118*(11), 5380–5552. https://doi.org/10.1002/jgrd.50171

Brock, C. A., Williamson, C., Kupc, A., Froyd, K. D., Erdesz, F., Wagner, N., et al. (2019). Aerosol size distributions during the Atmospheric Tomography Mission (ATom): Methods, uncertainties, and data products. *Atmospheric Measurement Techniques*, *12*(6), 3081–3099. https://doi.org/10.5194/amt-12-3081-2019

Canagaratna, M. R., Jayne, J. T., Jimenez, J. L., Allan, J. D., Alfarra, M. R., Zhang, Q., et al. (2007). Chemical and microphysical characterization of ambient aerosols with the aerodyne aerosol mass spectrometer. *Mass Spectrometry Reviews*, *26*(2), 185–222. https://doi.org/10.1002/mas.20115

Cheng, B., Wang-Li, L., Meskhidze, N., Classen, J., & Bloomfield, P. (2021). Partitioning of $NH_3-NH_4^+$ in the Southeastern U.S. *Atmosphere*, *12*, 1681. https://doi.org/10.3390/atmos12121681

Chin, M., Ginoux, P., Kinne, S., Torres, O., Holben, B. N., Duncan, B. N., et al. (2002). Tropospheric optical thickness from the GOCART model and comparisons with satellite and Sun photometer measurements. *Journal of the Atmospheric Sciences*, *59*, 461–483. https://doi.org/10.1175/1520-0469(2002)059<0461:taotft>2.0.co;2

Chung, S. H., & Seinfeld, J. H. (2002). Global distribution and climate forcing of carbonaceous aerosols. *Journal of Geophysical Research: Atmospheres*, *107*(D19), 4407. https://doi.org/10.1029/2001jd001397

Clarke, A. D., Collins, W. G., Rasch, P. J., Kapustin, V. N., Moore, K., Howell, S., & Fuelberg, H. E. (2001). Dust and pollution transport on global scales: Aerosol measurements and model predictions. *Journal of Geophysical Research*, *106*(D23), 32555–32570. https://doi.org/10.1029/2000jd900842

Cohen, A. J., Brauer, M., Burnett, R., Anderson, H. R., Frostad, J., Estep, K., et al. (2017). Estimates and 25-year trends of the global burden of disease attributable to ambient air pollution: An analysis of data from the Global Burden of Diseases Study 2015. *The Lancet*, *389*(10082), 1907–1918. https://doi.org/10.1016/s0140-6736(17)30505-6

Cooke, W. F., Liousse, C., Cachier, H., & Feichter, J. (1999). Construction of a 1° × 1° fossil fuel emission data set for carbonaceous aerosol and implementation and radiative impact in the ECHAM4 model. *Journal of Geophysical Research: Atmospheres*, *104*(D18), 22137–22162. https://doi.org/10.1029/1999jd900187

De Carlo, P. F., Kimmel, J. R., Trimborn, A., Northway, M. J., Jayne, J. T., Aiken, A. C., et al. (2006). Field-deployable, high-resolution, time-of-flight aerosol mass spectrometer. *Analytical Chemistry*, *78*(24), 8281–8289. https://doi.org/10.1021/ac061249n

Fairlie, T. D., Jacob, D. J., & Park, R. J. (2007). The impact of transpacific transport of mineral dust in the United States. *Atmospheric Environment*, *41*(6), 1251–1266. https://doi.org/10.1016/j.atmosenv.2006.09.048

Fountoukis, C., & Nenes, A. (2007). ISORROPIA II: A computationally efficient thermodynamic equilibrium model for $K^+-Ca^{2+}-Mg^{2+}-NH_4^+-Na^+-SO_4^{2-}-NO_3^--Cl^--H_2O$ aerosols. *Atmospheric Chemistry and Physics*, *7*(17), 4639–4659. https://doi.org/10.5194/acp-7-4639-2007

Giglio, L., Randerson, J. T., & Werf, G. R. (2013). Analysis of daily, monthly, and annual burned area using the fourth-generation global fire emissions database (GFED4). *Journal of Geophysical Research: Biogeosciences*, *118*(1), 317–328. https://doi.org/10.1002/jgrg.20042

Giorgi, F., & Chameides, W. L. (1986). Rainout lifetimes of highly soluble aerosols and gases as inferred from simulations with a general circulation model. *Journal of Geophysical Research: Atmospheres*, *91*(D13), 14367–14376. https://doi.org/10.1029/jd091id13p14367

Gließ, J., Mortier, A., Schulz, M., Andrews, E., Balkanski, Y., Bauer, S. E., et al. (2021). AeroCom phase III multi-model evaluation of the aerosol life cycle and optical properties using ground- and space-based remote sensing as well as surface in situ observations. *Atmospheric Chemistry and Physics*, *21*(1), 87–128. https://doi.org/10.5194/acp-21-87-2021

Graustein, W. C., & Turekian, K. K. (1986). 210Pb and 137Cs in air and soils measure the rate and vertical profile of aerosol scavenging. *Journal of Geophysical Research: Atmospheres*, *91*(D13), 14355–14366. https://doi.org/10.1029/jd091id13p14355

Grosjean, D., & Friedlander, S. K. (1975). Gas-particle distribution factors for organic and other pollutants in the Los Angeles Atmosphere. *Journal of the Air Pollution Control Association*, *25*(10), 1038–1044. https://doi.org/10.1080/00022470.1975.10470176

Guenther, A. B., Jiang, X., Heald, C. L., Sakulyanontvittaya, T., Duhl, T., Emmons, L. K., & Wang, X. (2012). The Model of Emissions of Gases and Aerosols from Nature version 2.1 (MEGAN2.1): An extended and updated framework for modeling biogenic emissions. *Geoscientific Model Development*, *5*(6), 1471–1492. https://doi.org/10.5194/gmd-5-1471-2012

Guo, H., Campuzano-Jost, P., Nault, B. A., Day, D. A., Schroder, J. C., Dibb, J. E., et al. (2021). The importance of size ranges in aerosol instrument intercomparisons: A case study for the ATom mission. *Atmospheric Measurement Techniques*, *14*, 3631–3655. https://doi.org/10.5194/amt-14-3631-2021

Guo, H., Otjes, R., Schlag, P., Kiendler-Scharr, A., Nenes, A., & Weber, R. J. (2018). Effectiveness of ammonia reduction on control of fine particle nitrate. *Atmospheric Chemistry and Physics*, *18*, 12241–12256. https://doi.org/10.5194/acp-18-12241-2018

Heald, C. L., Coe, H., Jimenez, J. L., Weber, R. J., Bahreini, R., Middlebrook, A. M., et al. (2011). Exploring the vertical profile of atmospheric organic aerosol: Comparing 17 aircraft field campaigns with a global model. *Atmospheric Chemistry and Physics*, *11*(24), 12673–12696. https://doi.org/10.5194/acp-11-12673-2011

Heald, C. L., Collett, J. L., Jr., Lee, T., Benedict, K. B., Schwandner, F. M., Li, Y., et al. (2012). Atmospheric ammonia and particulate inorganic nitrogen over the United States. *Atmospheric Chemistry and Physics*, *12*(21), 10295–10312. https://doi.org/10.5194/acp-12-10295-2012

Heald, C. L., Jacob, D. J., Park, R. J., Alexander, B., Fairlie, T. D., Yantosca, R. M., & Chu, D. A. (2006). Transpacific transport of Asian anthropogenic aerosols and its impact on surface air quality in the United States. *Journal of Geophysical Research: Atmospheres*, *111*(D14), D14310. https://doi.org/10.1029/2005jd006847

Heald, C. L., Jacob, D. J., Park, R. J., Russell, L. M., Huebert, B. J., Seinfeld, J. H., et al. (2005). A large organic aerosol source in the free troposphere missing from current models. *Geophysical Research Letters*, *32*(18), L18809. https://doi.org/10.1029/2005gl023831

Heald, C. L., Kroll, J. H., Jimenez, J. L., Docherty, K. S., De Carlo, P. F., Aiken, A. C., et al. (2010). A simplified description of the evolution of organic aerosol composition in the atmosphere. *Geophysical Research Letters*, *37*(8), L08803. https://doi.org/10.1029/2010gl042737

Henzing, J. S., Olivié, D. J. L., & van Velthoven, P. F. J. (2006). A parameterization of size resolved below cloud scavenging of aerosols by rain. *Atmospheric Chemistry and Physics*, *6*, 3363–3375. https://doi.org/10.5194/acp-6-3363-2006

Hodzic, A., Campuzano-Jost, P., Bian, H., Chin, M., Colarco, P. R., Day, D. A., et al. (2020). Characterization of organic aerosol across the global remote troposphere: A comparison of ATom measurements and global chemistry models. *Atmospheric Chemistry and Physics*, *20*(8), 4607–4635. https://doi.org/10.5194/acp-20-4607-2020

Hodzic, A., Jimenez, J. L., Madronich, S., Aiken, A. C., Bessagnet, B., Curci, G., et al. (2009). Modeling organic aerosols during MILAGRO: Importance of biogenic secondary organic aerosols. *Atmospheric Chemistry and Physics*, *9*(18), 6949–6981. https://doi.org/10.5194/acp-9-6949-2009

Hodzic, A., Kasibhatla, P. S., Jo, D. S., Cappa, C. D., Jimenez, J. L., Madronich, S., & Park, R. J. (2016). Rethinking the global secondary organic aerosol (SOA) budget: Stronger production, faster removal, shorter lifetime. *Atmospheric Chemistry and Physics*, *16*(12), 7917–7941. https://doi.org/10.5194/acp-16-7917-2016

Hodzic, A., Madronich, S., Kasibhatla, P. S., Tyndall, G., Aumont, B., Jimenez, J. L., et al. (2015). Organic photolysis reactions in tropospheric aerosols: Effect on secondary organic aerosol formation and lifetime. *Atmospheric Chemistry and Physics*, *15*(16), 9253–9269. https://doi.org/10.5194/acp-15-9253-2015

Hoesly, R. M., Smith, S. J., Feng, L., Klimont, Z., Janssens-Maenhout, G., Pitkanen, T., et al. (2018). Historical (1750–2014) anthropogenic emissions of reactive gases and aerosols from the Community Emissions Data System (CEDS). *Geoscientific Model Development*, *11*(1), 369–408. https://doi.org/10.5194/gmd-11-369-2018

Jacob, D. J., Liu, H., Mari, C., & Yantosca, R. M. (2000). Harvard wet deposition scheme for GMI (Vol. *6*). Retrieved from http://acmg.seas.harvard.edu/geos/wiki_docs/deposition/wetdep.jacob_et_al._2000.pdf

Jaeglé, L., Quinn, P. K., Bates, T. S., Alexander, B., & Lin, J.-T. (2011). Global distribution of sea salt aerosols: New constraints from in situ and remote sensing observations. *Atmospheric Chemistry and Physics*, *11*(7), 3137–3157. https://doi.org/10.5194/acp-11-3137-2011

Jimenez, J. L., Campuzano-Jost, P., Day, D. A., Nault, B. A., Price, D. J., & Schroder, J. C. (2019). *ATom: L2 measurements from CU high-resolution aerosol mass spectrometer (HR-AMS)*. ORNL DAAC. https://doi.org/10.3334/ORNLDAAC/1716

Jordan, C. E., Dibb, J. E., Anderson, B. E., & Fuelberg, H. E. (2003). Uptake of nitrate and sulfate on dust aerosols during TRACE-P. *Journal of Geophysical Research*, *108*(D21), 8817. https://doi.org/10.1029/2002JD003101

Katich, J. M., Samset, B. H., Bui, T. P., Dollner, M., Froyd, K. D., Campuzano-Jost, P., et al. (2018). Strong contrast in remote black carbon aerosol loadings between the Atlantic and Pacific basins. *Journal of Geophysical Research: Atmospheres*, *123*(23), 13386–13395. https://doi.org/10.1029/2018jd029206

Keller, C. A., Long, M. S., Yantosca, R. M., Silva, A. M. D., Pawson, S., & Jacob, D. J. (2014). HEMCO v1.0: A versatile, ESMF-compliant component for calculating emissions in atmospheric models. *Geoscientific Model Development*, *7*(4), 1409–1417. https://doi.org/10.5194/gmd-7-1409-2014

Koch, D., Schulz, M., Kinne, S., McNaughton, C., Spackman, J. R., Balkanski, Y., et al. (2009). Evaluation of black carbon estimations in global aerosol models. *Atmospheric Chemistry and Physics*, *9*(22), 9001–9026. https://doi.org/10.5194/acp-9-9001-2009

Kuhns, H., Knipping, E. M., & Vukovich, J. M. (2005). Development of a United States–Mexico emissions inventory for the big bend region-al aerosol and visibility observational (BRAVO) study. *Journal of the Air and Waste Management Association*, *55*(5), 677–692. https://doi.org/10.1080/10473289.2005.10464648

Laakso, L., Grönholm, T., Rannik, U., Kosmale, M., Fiedler, V., Vehkamäki, H., & Kulmala, M. (2003). Ultrafine particle scavenging coefficients calculated from 6 years field measurements. *Atmospheric Environment*, *37*, 3605–3613. https://doi.org/10.1016/s1352-2310(03)00326-1

Leibensperger, E. M., Mickley, L. J., Jacob, D. J., Chen, W.-T., Seinfeld, J. H., Nenes, A., et al. (2012). Climatic effects of 1950–2050 changes in US anthropogenic aerosols – Part 1: Aerosol trends and radiative forcing. *Atmospheric Chemistry and Physics*, *12*(7), 3333–3348. https://doi.org/10.5194/acp-12-3333-2012

Li, M., Zhang, Q., Kurokawa, J., Woo, J.-H., He, K., Lu, Z., et al. (2017). Mix: A mosaic Asian anthropogenic emission inventory under the international collaboration framework of the MICS-Asia and HTAP. *Atmospheric Chemistry and Physics*, *17*(2), 935–963. https://doi.org/10.5194/acp-17-935-2017

Liu, H., Jacob, D. J., Bey, I., & Yantosca, R. M. (2001). Constraints from 210Pb and 7Be on wet deposition and transport in a global three-dimensional chemical tracer model driven by assimilated meteorological fields. *Journal of Geophysical Research: Atmospheres*, *106*(D11), 12109–12128. https://doi.org/10.1029/2000jd900839

Liu, M., & Matsui, H. (2021). Improved simulations of global black carbon distributions by modifying wet scavenging processes in convective and mixed-phase clouds. *Journal of Geophysical Research: Atmospheres*, *126*, e2020JD033890. https://doi.org/10.1029/2020JD033890

Liu, X., Easter, R. C., Ghan, S. J., Zaveri, R., Rasch, P., Shi, X., et al. (2012). Toward a minimal representation of aerosols in climate models: Description and evaluation in the Community Atmosphere Model CAM5. *Geoscientific Model Development*, *5*(3), 709–739. https://doi.org/10.5194/gmd-5-709-2012

Luo, G., Yu, F., & Moch, J. M. (2020). Further improvement of wet process treatments in GEOS-Chem v12.6.0: Impact on global distributions of aerosols and aerosol precursors. *Geoscientific Model Development*, *13*(6), 2879–2903. https://doi.org/10.5194/gmd-13-2879-2020

Luo, G., Yu, F., & Schwab, J. (2019). Revised treatment of wet scavenging processes dramatically improves GEOS-Chem 12.0.0 simulations of surface nitric acid, nitrate, and ammonium over the United States. *Geoscientific Model Development*, *12*(8), 3439–3447. https://doi.org/10.5194/gmd-12-3439-2019

Malm, W. C., Sisler, J. F., Huffman, D., Eldred, R. A., & Cahill, T. A. (1994). Spatial and seasonal trends in particle concentration and optical extinction in the United States. *Journal of Geophysical Research: Atmospheres*, *99*(D1), 1347–1370. https://doi.org/10.1029/93jd02916

Mao, J., Paulot, F., Jacob, D. J., Cohen, R. C., Crounse, J. D., Wennberg, P. O., et al. (2013). Ozone and organic nitrates over the eastern United States: Sensitivity to isoprene chemistry. *Journal of Geophysical Research: Atmospheres*, *118*(19), 11256–11268. https://doi.org/10.1002/jgrd.50817

Marais, E. A., Jacob, D. J., Jimenez, J. L., Campuzano-Jost, P., Day, D. A., Hu, W., et al. (2016). Aqueous-phase mechanism for secondary organic aerosol formation from isoprene: Application to the southeast United States and co-benefit of SO2 emission controls. *Atmospheric Chemistry and Physics*, *16*(3), 1603–1618. https://doi.org/10.5194/acp-16-1603-2016

Marais, E. A., & Wiedinmyer, C. (2016). Air quality impact of diffuse and inefficient combustion emissions in Africa (DICE-Africa). *Environmental Science and Technology*, *50*(19), 10739–10745. https://doi.org/10.1021/acs.est.6b02602

Martell, E. A., & Moore, H. E. (1974). Tropospheric residence times: A critical review. *Journal de Recherches Atmospheriques*, *8*, 903–910.

Martin, R. V., Jacob, D. J., Yantosca, R. M., Chin, M., & Ginoux, P. (2003). Global and regional decreases in tropospheric oxidants from photochemical effects of aerosols. *Journal of Geophysical Research: Atmospheres*, *108*(D3), 4097. https://doi.org/10.1029/2002jd002622

Maxwell-Meier, K., Weber, R., Song, C., Orsini, D., Ma, Y., Carmichael, G. R., & Streets, D. G. (2004). Inorganic composition of fine particles in mixed mineral dust – Pollution plumes observed from airborne measurements during ACE-Asia. *Journal of Geophysical Research*, *109*, D19S07. https://doi.org/10.1029/2003JD004464

Miller, C. C., Jacob, D. J., Marais, E. A., Yu, K., Travis, K. R., Kim, P. S., et al. (2017). Glyoxal yield from isoprene oxidation and relation to formaldehyde: Chemical mechanism, constraints from SENEX aircraft observations, and interpretation of OMI satellite data. *Atmospheric Chemistry and Physics*, *17*(14), 8725–8738. https://doi.org/10.5194/acp-17-8725-2017

Nah, T., Guo, H., Sullivan, A. P., Chen, Y., Tanner, D. J., Nenes, A., et al. (2018). Characterization of aerosol composition, aerosol acidity, and organic acid partitioning at an agriculturally intensive rural southeastern US site. *Atmospheric Chemistry and Physics*, *18*, 11471–11491. https://doi.org/10.5194/acp-18-11471-2018

Nault, B. A., Campuzano-Jost, P., Day, D. A., Jo, D. S., Schroder, J. C., Allen, H. M., et al. (2021). Chemical transport models often underestimate inorganic aerosol acidity in remote regions of the atmosphere. *Communications Earth & Environment*, *2*(1), 93. https://doi.org/10.1038/s43247-021-00164-0

Nault, B. A., Campuzano-Jost, P., Day, D. A., Schroder, J. C., Anderson, B., Beyersdorf, A. J., et al. (2018). Secondary organic aerosol production from local emissions dominates the organic aerosol budget over Seoul, South Korea, during KORUS-AQ. *Atmospheric Chemistry and Physics*, *18*(24), 17769–17800. https://doi.org/10.5194/acp-18-17769-2018

O'Brien, R. E., & Kroll, J. H. (2019). Photolytic aging of secondary organic aerosol: Evidence for a substantial photo-recalcitrant fraction. *The Journal of Physical Chemistry Letters*, *10*(14), 4003–4009. https://doi.org/10.1021/acs.jpclett.9b01417

Pai, S. J., Heald, C. L., Pierce, J. R., Farina, S. C., Marais, E. A., Jimenez, J. L., et al. (2020). An evaluation of global organic aerosol schemes using airborne observations. *Atmospheric Chemistry and Physics*, *20*(5), 2637–2665. https://doi.org/10.5194/acp-20-2637-2020

Pang, Y., Turpin, B. J., & Gundel, L. A. (2006). On the importance of organic oxygen for understanding organic aerosol particles. *Aerosol Science and Technology*, *40*(2), 128–133. https://doi.org/10.1080/02786820500423790

Park, R. J., Jacob, D. J., Chin, M., & Martin, R. V. (2003). Sources of carbonaceous aerosols over the United States and implications for natural visibility. *Journal of Geophysical Research: Atmospheres*, *108*(D12), 4355. https://doi.org/10.1029/2002jd003190

Park, R. J., Jacob, D. J., Field, B. D., Yantosca, R. M., & Chin, M. (2004). Natural and transboundary pollution influences on sulfate-nitrate-ammonium aerosols in the United States: Implications for policy. *Journal of Geophysical Research: Atmospheres*, *109*(D15), D15204. https://doi.org/10.1029/2003jd004473

Philip, S., Martin, R. V., & Keller, C. A. (2016). Sensitivity of chemistry-transport model simulations to the duration of chemical and transport operators: A case study with GEOS-Chem v10-01. *Geoscientific Model Development*, *9*(5), 1683–1695. https://doi.org/10.5194/gmd-9-1683-2016

Philip, S., Martin, R. V., Pierce, J. R., Jimenez, J. L., Zhang, Q., Canagaratna, M. R., et al. (2014). Spatially and seasonally resolved estimate of the ratio of organic mass to organic carbon. *Atmospheric Environment*, *87*, 34–40. https://doi.org/10.1016/j.atmosenv.2013.11.065

Price, H. U., Jaffe, D. A., Doskey, P. V., McKendry, I., & Anderson, T. L. (2003). Vertical profiles of O3, aerosols, CO and NMHCs in the northeast Pacific during the TRACE-P and ACE-Asia experiments. *Journal of Geophysical Research*, *108*(D20), 8799. https://doi.org/10.1029/2002JD002930

Pye, H. O. T., Liao, H., Wu, S., Mickley, L. J., Jacob, D. J., Henze, D. K., & Seinfeld, J. H. (2009). Effect of changes in climate and emissions on future sulfate-nitrate-ammonium aerosol levels in the United States. *Journal of Geophysical Research: Atmospheres*, *114*(D1), D01205. https://doi.org/10.1029/2008jd010701

Pye, H. O. T., & Seinfeld, J. H. (2010). A global perspective on aerosol from low-volatility organic compounds. *Atmospheric Chemistry and Physics*, *10*(9), 4377–4401. https://doi.org/10.5194/acp-10-4377-2010

Rastigejev, Y., Park, R., Brenner, M. P., & Jacob, D. J. (2010). Resolving intercontinental pollution plumes in global models of atmospheric transport. *Journal of Geophysical Research*, *115*(D2), D02302. https://doi.org/10.1029/2009jd012568

Ridley, D. A., Heald, C. L., & Ford, B. (2012). North African dust export and deposition: A satellite and model perspective. *Journal of Geophysical Research: Atmospheres*, *117*(D2), D02202. https://doi.org/10.1029/2011jd016794

Samset, B. H., Myhre, G., Herber, A., Kondo, Y., Li, S.-M., Moteki, N., et al. (2014). Modelled black carbon radiative forcing and atmospheric lifetime in AeroCom Phase II constrained by aircraft observations. *Atmospheric Chemistry and Physics*, *14*(22), 12465–12477. https://doi.org/10.5194/acp-14-12465-2014

Schroder, J. C., Campuzano-Jost, P., Day, D. A., Shah, V., Larson, K., Sommers, J. M., et al. (2018). Sources and secondary production of organic aerosols in the Northeastern United States during WINTER. *Journal of Geophysical Research: Atmospheres*, *123*(14), 7771–7796. https://doi.org/10.1029/2018jd028475

Schulz, M., Textor, C., Kinne, S., Balkanski, Y., Bauer, S., Berntsen, T., et al. (2006). Radiative forcing by aerosols as derived from the Aero-Com present-day and pre-industrial simulations. *Atmospheric Chemistry and Physics*, *6*, 5225–5246. https://doi.org/10.5194/acp-6-5225-2006

Schwarz, J. P., Weinzierl, B., Samset, B. H., Dollner, M., Heimerl, K., Markovic, M. Z., et al. (2017). Aircraft measurements of black carbon vertical profiles show upper tropospheric variability and stability. *Geophysical Research Letters*, *44*(2), 1132–1140. https://doi.org/10.1002/2016gl071241

Seinfeld, J. H., & Pandis, S. N. (2016). *Atmospheric chemistry and physics* (3rd ed.). Wiley-Interscience.

Shan, Y., Liu, X., Lin, L., Ke, Z., & Lu, Z. (2021). An improved representation of aerosol wet removal by deep convection and impacts on simulated aerosol vertical profiles. *Journal of Geophysical Research: Atmospheres*, *126*, e2020JD034173. https://doi.org/10.1029/2020JD034173

Sherwen, T., Schmidt, J. A., Evans, M. J., Carpenter, L. J., Großmann, K., Eastham, S. D., et al. (2016). Global impacts of tropospheric halogens (Cl, Br, I) on oxidants and composition in GEOS-Chem. *Atmospheric Chemistry and Physics*, *16*(18), 12239–12271. https://doi.org/10.5194/acp-16-12239-2016

Strode, S. A., Duncan, B. N., Yegorova, E. A., Kouatchou, J., Ziemke, J. R., & Douglass, A. R. (2015). Implications of carbon monoxide bias for methane lifetime and atmospheric composition in chemistry climate models. *Atmospheric Chemistry and Physics*, *15*(20), 11789–11805. https://doi.org/10.5194/acp-15-11789-2015

Textor, C., Schulz, M., Guibert, S., Kinne, S., Balkanski, Y., Bauer, S., et al. (2006). Analysis and quantification of the diversities of aerosol life cycles within AeroCom. *Atmospheric Chemistry and Physics*, *6*(7), 1777–1813. https://doi.org/10.5194/acp-6-1777-2006

Tilmes, S., Hodzic, A., Emmons, L. K., Mills, M. J., Gettelman, A., Kinnison, D. E., et al. (2019). Climate forcing and trends of organic aerosols in the Community Earth System Model (CESM2). *Journal of Advances in Modeling Earth Systems*, *11*(12), 4323–4351. https://doi.org/10.1029/2019ms001827

Travis, K. R., Jacob, D. J., Fisher, J. A., Kim, P. S., Marais, E. A., Zhu, L., et al. (2016). Why do models overestimate surface ozone in the Southeast United States? *Atmospheric Chemistry and Physics*, *16*(21), 13561–13577. https://doi.org/10.5194/acp-16-13561-2016

Tsigaridis, K., Daskalakis, N., Kanakidou, M., Adams, P. J., Artaxo, P., Bahadur, R., et al. (2014). The AeroCom evaluation and intercomparison of organic aerosol in global models. *Atmospheric Chemistry and Physics*, *14*(19), 10845–10895. https://doi.org/10.5194/acp-14-10845-2014

Turpin, B. J., & Lim, H.-J. (2001). Species contributions to PM2.5 mass concentrations: Revisiting common assumptions for estimating organic mass. *Aerosol Science and Technology*, *35*(1), 602–610. https://doi.org/10.1080/02786820119445

Walker, J. M., Philip, S., Martin, R. V., & Seinfeld, J. H. (2012). Simulation of nitrate, sulfate, and ammonium aerosols over the United States. *Atmospheric Chemistry and Physics*, *12*(22), 11213–11227. https://doi.org/10.5194/acp-12-11213-2012

Wang, H., Easter, R. C., Rasch, P. J., Wang, M., Liu, X., Ghan, J., et al. (2013). Sensitivity of remote aerosol distributions to representation of cloud-aerosol interactions in a global climate model. *Geoscientific Model Development*, 765–782. https://doi.org/10.5194/gmd-6-765-2013

Wang, Q., Jacob, D. J., Fisher, J. A., Mao, J., Leibensperger, E. M., Carouge, C. C., et al. (2011). Sources of carbonaceous aerosols and deposited black carbon in the Arctic in winter-spring: Implications for radiative forcing. *Atmospheric Chemistry and Physics*, *11*(23), 12453–12473. https://doi.org/10.5194/acp-11-12453-2011

Wang, Q., Jacob, D. J., Spackman, J. R., Perring, A. E., Schwarz, J. P., Moteki, N., et al. (2014). Global budget and radiative forcing of black carbon aerosol: Constraints from pole-to-pole (HIPPO) observations across the Pacific. *Journal of Geophysical Research: Atmospheres*, *119*(1), 195–206. https://doi.org/10.1002/2013jd020824

Wang, X., Heald, C. L., Ridley, D. A., Schwarz, J. P., Spackman, J. R., Perring, A. E., et al. (2014). Exploiting simultaneous observational constraints on mass and absorption to estimate the global direct radiative forcing of black carbon and brown carbon. *Atmospheric Chemistry and Physics*, *14*(20), 10989–11010. https://doi.org/10.5194/acp-14-10989-2014

Wang, X., Zhang, L., & Moran, M. D. (2010). Uncertainty assessment of current size-resolved parameterizations for below-cloud particle scavenging by rain. *Atmospheric Chemistry and Physics*, *10*, 5685–5705. https://doi.org/10.5194/acp-10-5685-2010

Wang, X., Zhang, L., & Moran, M. D. (2014). Development of a new semi-empirical parameterization for below-cloud scavenging of size-resolved aerosol particles by both rain and snow. *Geoscientific Model Development*, *7*(3), 799–819. https://doi.org/10.5194/gmd-7-799-2014

Wang, Y., Xia, W., Liu, X., Xie, S., Lin, W., Tang, Q., et al. (2021). Disproportionate control on aerosol burden by light rain. *Nature Geoscience*, *14*(2), 72–76. https://doi.org/10.1038/s41561-020-00675-z

Wesely, M. L. (1989). Parameterization of surface resistances to gaseous dry deposition in regional-scale numerical models. *Atmospheric Environment*, *23*(6), 1293–1304. https://doi.org/10.1016/0004-6981(89)90153-4

White, W. H., & Roberts, P. T. (1977). On the nature and origins of visibility-reducing aerosols in the los angeles air basin. *Atmospheric Environment*, *11*(9), 803–812. https://doi.org/10.1016/0004-6981(77)90042-7

Williamson, C. J., Kupc, A., Axisa, D., Bilsback, K. R., Bui, T., Campuzano-Jost, P., et al. (2019). A large source of cloud condensation nuclei from new particle formation in the tropics. *Nature*, *574*(7778), 399–403. https://doi.org/10.1038/s41586-019-1638-9

Wofsy, S. C., Afshar, S., Allen, H. M., Apel, E., Asher, E. C., Barletta, B., et al. (2018). ATom: Merged atmospheric chemistry, trace gases, and aerosols [Dataset]. ORNL DAAC. https://doi.org/10.3334/ORNLDAAC/1581

Yu, P., Froyd, K. D., Portmann, R. W., Toon, O. B., Freitas, S. R., Bardeen, C. G., et al. (2019). Efficient in-cloud removal of aerosols by deep convection. *Geophysical Research Letters*, *46*(2), 1061–1069. https://doi.org/10.1029/2018gl080544

Zakoura, M., & Pandis, S. N. (2018). Overprediction of aerosol nitrate by chemical transport models: The role of grid resolution. *Atmospheric Environment*, *187*, 390–400. https://doi.org/10.1016/j.atmosenv.2018.05.066

Zawadowicz, M. A., Lee, B. H., Shrivastava, M., Zelenyuk, A., Zaveri, R. A., Flynn, C., et al. (2020). Photolysis controls atmospheric budgets of biogenic secondary organic aerosol. *Environmental Science & Technology*, *54*(7), 3861–3870. https://doi.org/10.1021/acs.est.9b07051

Zhang, L., Gong, S., Padro, J., & Barrie, L. (2001). A size-segregated particle dry deposition scheme for an atmospheric aerosol module. *Atmospheric Environment*, *35*(3), 549–560. https://doi.org/10.1016/s1352-2310(00)00326-5

Zhang, L., Jacob, D. J., Knipping, E. M., Kumar, N., Munger, J. W., Carouge, C. C., et al. (2012). Nitrogen deposition to the United States: Distribution, sources, and processes. *Atmospheric Chemistry and Physics*, *12*, 4539–4554. https://doi.org/10.5194/acp-12-4539-2012

Zhang, Q., Worsnop, D. R., Canagaratna, M. R., & Jimenez, J. L. (2005). Hydrocarbon-like and oxygenated organic aerosols in Pittsburgh: Insights into sources and processes of organic aerosols. *Atmospheric Chemistry and Physics*, *5*(12), 3289–3311. https://doi.org/10.5194/acp-5-3289-2005